

High temperature piezoelectric ceramics in the $\text{Bi}(\text{Mg}_{1/2}\text{Ti}_{1/2})\text{O}_3\text{-BiFeO}_3\text{-BiScO}_3\text{-PbTiO}_3$ system

Tutu Sebastian · Iasmi Sterianou · Derek C. Sinclair · Andrew J. Bell · David A. Hall · Ian M. Reaney

Received: 13 March 2009 / Accepted: 15 March 2010 / Published online: 27 March 2010
© Springer Science+Business Media, LLC 2010

Abstract Compositions in the pseudoquaternary system, $1-x(0.35\text{Bi}(\text{Mg}_{1/2}\text{Ti}_{1/2})\text{O}_3-0.30\text{BiFeO}_3-0.35\text{BiScO}_3)-x\text{PbTiO}_3$ were fabricated and characterised at the morphotropic phase boundary (MPB) between ferroelectric rhombohedral and tetragonal phases. The MPB occurred at $x \approx 0.48$ at which composition the ferroelectric to paraelectric phase transition, $T_C=450^\circ\text{C}$, the piezoelectric constant, $d_{33}=328$ pC/N and electromechanical coupling factor, $k_p=0.44$. The piezoelectric properties are viable for actuator applications but lower than equivalent high T_C piezoelectrics such as $0.36\text{BiScO}_3-0.64\text{PbTiO}_3$ ($d_{33}=450$ pC/N, $T_C=450^\circ\text{C}$). However, the relative reduction in the Sc_2O_3 content gives a significant cost saving which may prove a commercial advantage.

Keywords Piezoelectrics · Morphotropic phase boundary · High curie temperature · BS-PT · BMTFS-PT

1 Introduction

Lead zirconate titanate (PZT) based piezoelectric ceramics have dominated the transducer and actuator industries since

their development in the early 1950's [1]. Typically, transducers and actuators make use of morphotropic phase boundary (MPB) compositions between rhombohedral (R) and tetragonal (T) phases in the PZT phase diagram at ~ 48 mol% PbTiO_3 [1]. However, environmental restrictions on the usage of lead and the depoling and ageing of PZT at temperatures above 200°C have focussed the attention of researchers worldwide to look for alternative materials [2]. In 2001, Eitel *et al* [3] reported a ceramic based on the solid solution, $\text{BiScO}_3\text{-PbTiO}_3$ (BS-PT) which had a lower concentration of PbO, higher Curie temperature, $T_C=450^\circ\text{C}$ compared with $<380^\circ\text{C}$ for PZT and a similar piezoelectric constant, $d_{33}=450$ pC/N. However, the high cost of Sc_2O_3 currently restricts its usage in commercial applications. Other $\text{Bi}(\text{Me})\text{O}_3\text{-PbTiO}_3$ systems have been studied extensively but the majority have shown either limited solid solubility, eg: $\text{BiInO}_3\text{-PbTiO}_3$ [4], $\text{BiGaO}_3\text{-PbTiO}_3$ [5] or inferior properties eg: $\text{Bi}(\text{Mg}_{1/2}\text{Ti}_{1/2})\text{O}_3\text{-PbTiO}_3$ [6], $\text{Bi}(\text{Mg}_{1/2}\text{Zr}_{1/2})\text{O}_3\text{-PbTiO}_3$ [7]. The only notable success in decreasing costs whilst sustaining usable piezoelectric activity was described in the work of Sterianou *et al* [8, 9] who substituted Sc_2O_3 with up to 80% Fe_2O_3 in the solid solution $(1-x)\text{Bi}(\text{Sc}_{1-y}\text{Fe}_y)\text{O}_3-x\text{PbTiO}_3$ (BSF-PT). However, piezoelectric properties significantly deteriorated for $y > 0.5$ due to partially immiscibility of the two perovskite compositions [9].

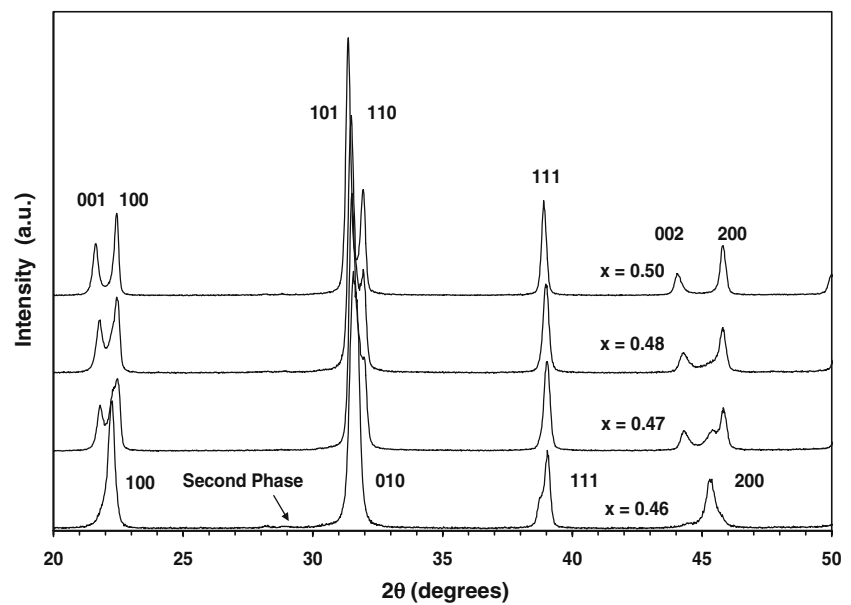
To overcome the problems of immiscibility encountered by Sterianou *et al* [9], the pseudoternary system BSF-PT has been expanded in this work to include $\text{Bi}(\text{Mg}_{1/2}\text{Ti}_{1/2})\text{O}_3$. To simplify the search for MPB compositions the ratio of $\text{BiMg}_{1/2}\text{Ti}_{1/2}\text{O}_3\text{:BiFeO}_3\text{:BiScO}_3$ has been initially fixed at 0.35:0.3:0.35. The objective of the work reported here is therefore to characterise compositions near the MPB in the solid solution $(1-x)(0.35\text{Bi}(\text{Mg}_{1/2}\text{Ti}_{1/2})\text{O}_3-0.3\text{BiFeO}_3-0.35\text{BiScO}_3)-x\text{PbTiO}_3$, $(1-x)\text{BMTFS}-x\text{PT}$ and determine whether such complex systems yield

T. Sebastian (✉) · I. Sterianou · D. C. Sinclair · I. M. Reaney
Department of Engineering Materials, University of Sheffield,
Sir Robert Hadfield Building,
Sheffield S1 3JD, UK
e-mail: mtq07ts@shef.ac.uk

A. J. Bell
Institute for Materials Research, University of Leeds,
Leeds LS2 9JT, UK

D. A. Hall
Materials Science Centre, School of Materials,
University of Manchester,
Grosvenor St.,
Manchester M1 7HS, UK

Fig. 1 X-ray diffraction traces of sintered pellets of $(1-x)\text{BMTFS}-x\text{PT}$ for $x=0.46, 0.47, 0.48$ and 0.50 . Peaks are indexed based on pseudo cubic cell



piezoelectric coefficients suitable for commercial applications whilst retaining $T_C \geq 450^\circ\text{C}$.

2 Experimental

Polycrystalline samples in the solid solution $(1-x)\text{BMTFS}-x\text{PT}$, $0.50 \geq x \geq 0.46$ were prepared using the solid state mixed oxide route. Bi_2O_3 (99.9%, Acros Organics, Geel, Belgium), PbO (99.9%, Acros Organics, Geel, Belgium), $\text{Mg}(\text{OH})_2$ (95%, Fisher Scientific, Loughborough, U.K), TiO_2 (99.9%, Sigma-Aldrich, Dorset, U.K), Fe_2O_3 (99% Aldrich Chemical company Inc. Milwaukee, U.S.A), Sc_2O_3 (99.99%, Stanford Materials Corporation, U.S.A) were weighed out in stoichiometric amounts in ~ 100 g batches to an accuracy of ~ 0.01 g and attrition milled using 3 mm diameter Y_2O_3 stabilised zirconia for 1 hour in distilled water. The milling media were removed and the remaining slurry was dried in an oven for 48 hours at 80°C . The dried sample was crushed using a mortar and pestle until it passed completely through a $355 \mu\text{m}$ mesh sieve. Powder was reacted at 900°C for 2 h in a lidded alumina crucible using a ramp rate of 2° per minute. The reacted powders were attrition milled for 1 hour in distilled water using yttria stabilised ZrO_2 milling media. The slurry was dried, crushed and sieved as before. Dried samples were pressed into 10 mm diameter pellets using a uniaxial press at ~ 1 tonne for ~ 1 min. Pellets and a small amount of powder of the same composition as that of pellet were placed on platinum foil and covered with a lid and sintered. The sacrificial powder was used to create a vapour pressure of the volatile species (PbO and Bi_2O_3) within the vicinity of the pellet. Sintering was carried out in air at $1,000^\circ\text{C}$ for 5 h at a ramp rate of 5° per minute.

X-ray diffraction was performed on a D500 Siemens diffractometer using $\text{Cu K}\alpha$ ($\lambda=1.540598 \text{ \AA}$) radiation to examine the phase purity of the system. Reflections were measured in steps of 0.02° at a speed of 0.1° per minute across the 2θ range 20 to 70° and data were analysed using ‘STOE WinXPow’ software. Surface morphology was examined using Scanning electron microscopy (SEM), (JEOL JSM6400) on thermally etched samples polished to $1 \mu\text{m}$.

Prior to measuring the dielectric, ferroelectric and piezoelectric properties, pellets were electroded with gold paste and fired at 800°C for 2 hours. Dielectric properties were measured between room temperature and 600°C using an inductance/capacitance/resistance (LCR) meter (4284A, HP). Relative dielectric permittivity (ϵ_r) and dielectric loss ($\tan \delta$) were measured at frequencies of 1, 10, 100 and

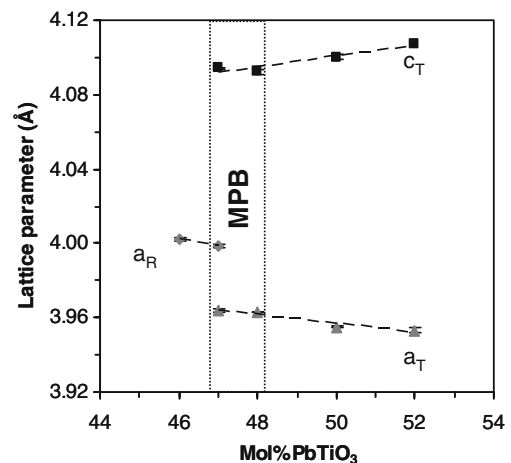


Fig. 2 Room temperature lattice parameters of $(1-x)\text{BMTFS}-x\text{PT}$ for $x=0.46, 0.47, 0.48, 0.50$ and 0.52 ceramics obtained from refinement of XRD data

Table 1 Piezoelectric properties of (1-x)BMTFS-xPT, compared with known reported ceramics.

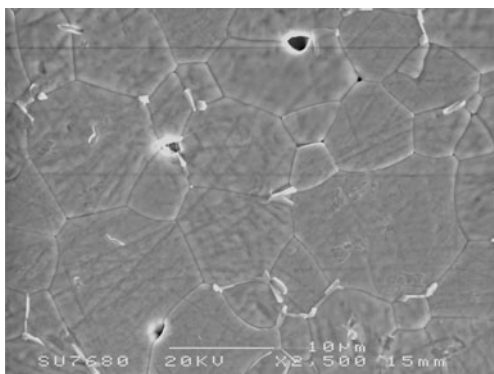
Material	T_C (°C)	$\tan \delta$	d_{33} (pC/N)	k_p	c_{T/a_T}	Reference
Undoped PZT	386	0.012	223	0.53	1.022	[1]
Navy type II (PZT)	365	0.017	374	0.60		[1]
0.36BiScO ₃ -0.64PbTiO ₃	450	0.027	460	0.56	1.023	[3]
0.63Bi(Mg _{1/2} Ti _{1/2})O ₃ -0.37PbTiO ₃	478	0.079	225	-	1.034	[6]
0.45Bi(Sc _{1/2} Fe _{1/2})O ₃ -0.55PbTiO ₃	440	0.033	298	0.49	1.021	[8]
Current work						
0.54BMFTS-0.46PT	440	0.033	183	0.18		
0.53BMFTS-0.47PT	443	0.025	226	0.27	1.0328	
0.52BMFTS-0.48PT	450	0.036	328	0.44	1.0327	
0.50BMFTS-0.50PT	463	0.019	270	0.31	1.0367	

250 kHz. Polarization-electric field (P-E) measurements were conducted in a heated silicone oil bath at a temperature of 100°C and a frequency of 2 Hz using a ferroelectric test system based on a HP33120A function generator in combination with a high voltage (+/- 5 kV) amplifier and a current amplifier. The piezoelectric constant, d_{33} , was measured using a Berlincourt meter (IAAS ZJ-2) on a pellet poled at 150°C in a silicone oil bath under optimum field (60 kV/cm) for 5 min. The electromechanical coupling factor, k_p was measured using an impedance analyzer (Agilent 4294A) based on IEEE standards [10]. Strain (S) was measured using a non-contact fibre-optic displacement probe (10 $\mu\text{m.V}^{-1}$ sensitivity, Philtec Inc) to generate strain-electric field loops.

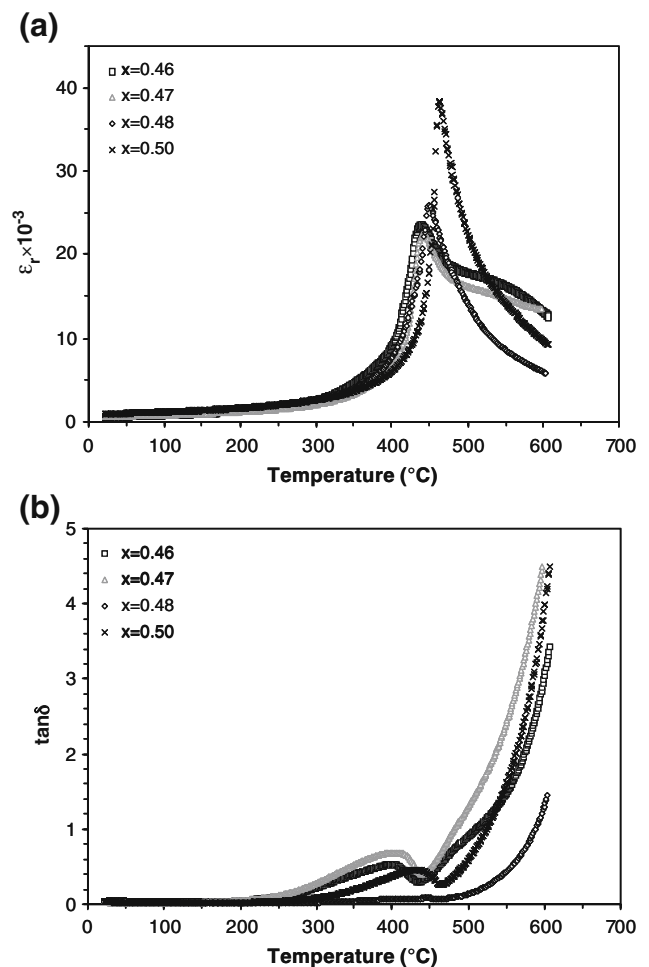
3 Results and discussion

3.1 Phase stability and microstructure

Figure 1 shows the XRD traces of pellets of all compositions sintered for 5 h. All major peaks could be attributed to perovskite-structured phases but minor unidentified second phase peaks appear at approximately $29^\circ 2\theta$ for $x \leq 0.46$

**Fig. 3** SEM image showing the grain structure of BMTFS-PT, $x=0.50$

compositions. Rhombohedral symmetry, characterised by splitting of the $\{111\}_p$ perovskite peak, was observed at room temperature for $x=0.46$. For $x > 0.47$ splitting of the $\{110\}_p$ peak show evidence of a structural phase transition to a tetragonally distorted perovskite structure. $\{200\}_p$

**Fig. 4** (a) Relative permittivity and (b) dielectric loss for sintered pellets of (1-x)BMTFS-xPT for $x=0.46$, 0.47, 0.48 and 0.50, at 10 kHz

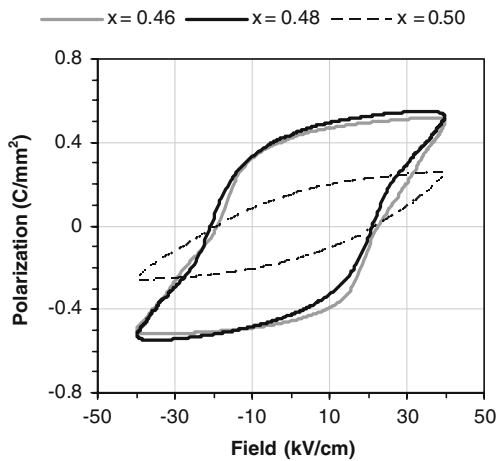


Fig. 5 Hysteresis curves obtained at 100°C for sintered pellets of (1-x)BMTFS-xPT for x=0.46, 0.48 and 0.50 at a frequency of 2 Hz

perovskite peaks show a clear evidence of structural transformation from rhombohedral to tetragonal phase with both phases co-existing at $x=0.47$, peaks at 2θ values 44.197° , 45.744° corresponding to tetragonal phase and at 45.304° corresponding to rhombohedral phase. It was concluded therefore that an MPB occurred in the BMTFS-PT system at $0.48 \geq x \geq 0.46$. Figure 2 presents room temperature lattice parameters for this system. The lattice parameters of tetragonal 0.52BMTFS-0.48PT were obtained as $a=3.9630(10)$ and $c=4.0925(13)$. The degree of tetragonal distortion denoted by (c_T / a_T) for various Bi (Me) O_3 -PbTiO₃ systems is shown in Table 1. The c/a ratio at MPB of the current system (~ 3%) is relatively high when compared to other systems. SEM images of thermally etched pellets across the MPB for $0.50 \geq x \geq 0.46$ revealed the grain size to be ~6-7 μm for all samples with no second phase, as typified by Fig. 3.

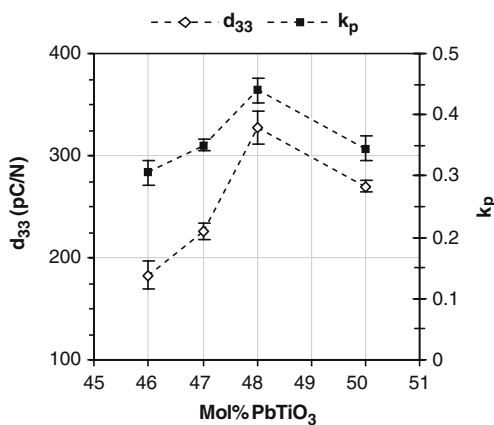


Fig. 6 Piezoelectric constant, d_{33} and electromechanical coupling factor, k_p near morphotropic phase boundary in (1-x)BMTFS-xPT, showing enhanced values at MPB

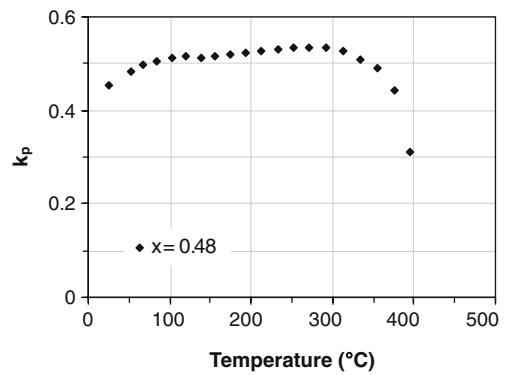


Fig. 7 Planar electromechanical coupling factor, k_p , versus temperature for a poled 0.52 BMTFS-0.48 PT ceramic

3.2 Electrical characterisation

Relative permittivity and dielectric loss versus temperature for unpoled samples at 10 kHz for $0.50 \geq x \geq 0.46$ are plotted in Fig. 4. All samples had $T_C \geq 440^\circ\text{C}$, considerably higher than that of PZT and equivalent to 0.63BS-0.37PT with dielectric loss < 0.04 at room temperature. However, a second anomaly was observed for $x=0.46$ at 550°C . Similar high temperature anomalies have been previously attributed to the immiscibility of perovskite phases, one of which is rich in PbTiO₃/BiFeO₃ with a high T_C [9]. The precise composition of these regions may only be determined by energy dispersive X-ray analysis of thin sections utilising transmission electron microscopy. This work is underway and will be presented elsewhere in a more detailed study of the ceramic microstructure. In the $(1-x)\text{BS}_y\text{F}_{(1-y)}\text{-xPT}$ system second high temperature phase transitions were encountered for $y < 0.5$ and for all values of x across the

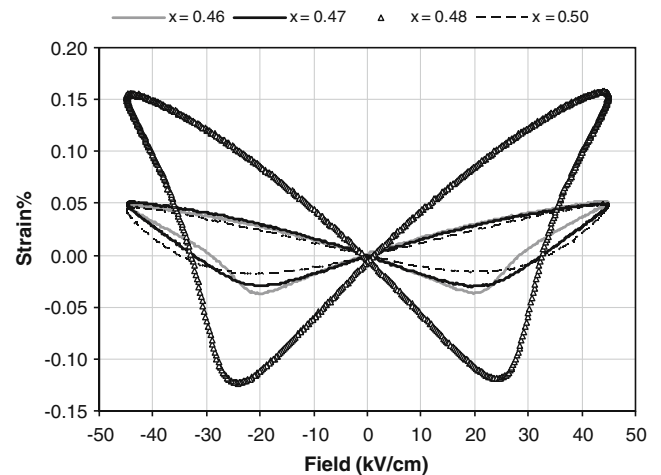


Fig. 8 Bipolar strain-electric field curves obtained at room temperature for sintered pellets of (1-x)BMTFS-xPT for x=0.46, 0.47, 0.48 and 0.50, at a frequency of 0.1 Hz

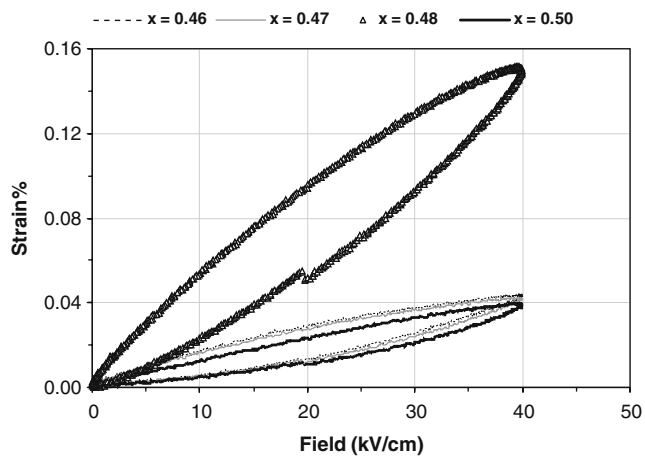


Fig. 9 Unipolar strain–electric field curves obtained at room temperature for sintered pellets of $(1-x)\text{BMTFS}-x\text{PT}$ for $x=0.46$, 0.47 , 0.48 and 0.50 , at a frequency of 0.1 Hz

MPB [9]. The immiscibility presented a thermodynamic barrier to ceramic homogeneity and prevented optimisation of the piezoelectric properties at the MPB. In contrast, in the BMTFS–PT system, the high temperature phase transition is absent for $x \geq 0.47$ and the addition of $\text{BiMg}_{1/2}\text{Ti}_{1/2}\text{O}_3$ to form a quaternary system has had the desired effect of suppressing immiscibility across the MPB.

Figure 5 shows the P–E hysteresis loops for $x=0.46$, 0.48 and 0.5 obtained at 100°C . Optimum $P_r \approx 43\ \mu\text{C}/\text{cm}^2$ and coercive field $E_c \approx 21\ \text{kV}/\text{cm}$ was achieved for $x=0.48$. The non-saturated P–E loop for $x=0.5$ is attributed to an increase in the coercive field associated with increased tetragonality, Fig. 2.

Figure 6 shows the d_{33} and k_p for $0.50 \geq x \geq 0.46$. d_{33} ($328\ \text{pC}/\text{N}$) and k_p (0.44) values are optimised in the tetragonal phase (Fig. 1) at $x=0.48$. In PZT, the piezoelectric response is also optimised in the tetragonal phase field in the vicinity of the MPB [1]. Figure 7 illustrates the thermal stability of the piezoelectric ceramic by measuring the variation of k_p as a function of temperature. It retains the room temperature k_p (~ 0.44) up to $\sim 375^\circ\text{C}$, considerably higher than PZT. Table 1 compares T_C , $\tan\delta$, d_{33} , k_p and c_T/a_T of BMTFS–PT compositions with the reported values for various piezoelectric compounds. d_{33} compares well with Navy type I ceramics but exhibits a higher T_C . However, ceramics in the solid solution BS–PT still show superior d_{33} for equivalent T_C although their higher Sc_2O_3 -content makes them commercially less appealing.

Figure 8 represents S–E response of compositions $0.50 \geq x \geq 0.46$ under bipolar drive for a maximum field of $45\ \text{kV}/\text{cm}$ and at a frequency of $0.1\ \text{Hz}$. Ceramics with $x=$

0.48 exhibit the maximum strain ($\sim 0.37\%$ at $55\ \text{kV}/\text{cm}$). Figure 9 shows the unipolar S–E curves for $0.50 \geq x \geq 0.46$ under the same conditions as the bipolar measurements. The maximum unipolar strain is exhibited by $x=0.48$ (~ 0.15) with a slope that gives an effective d_{33} of $\sim 380\ \text{pC}/\text{N}$.

4 Conclusions

$(1-x)\text{BMTFS}-x\text{PT}$ compositions have been fabricated in the search for a low cost commercially viable $\text{Bi}(\text{Me})\text{O}_3-\text{PbTiO}_3$ piezoelectric ceramic. The MPB occurs at $0.48 \geq x \geq 0.46$ and for $x=0.48$, $d_{33}=328\ \text{pC}/\text{N}$ with $T_C=450^\circ\text{C}$. To date, d_{33} is considerably higher for $0.36\text{BiScO}_3-0.64\text{PbTiO}_3$ ($450\ \text{pC}/\text{N}$) systems which have an equivalent T_C but the content of highly expensive Sc_2O_3 is significantly reduced in BMTFS–PT which may offer a commercial advantage. BMTFS–PT shows a cost reduction of about 45% compared to BS–PT, based on the laboratory scale production. Moreover, there is considerable potential in this quaternary system for a range of MPB compositions by altering the $\text{BiMg}_{1/2}\text{Ti}_{1/2}\text{O}_3:\text{BiFeO}_3:\text{BiScO}_3$ ratio. Future studies may therefore yield superior piezoelectric ceramics than reported here.

Acknowledgements The authors thank the Engineering and Physical Science Research Council (EP/E057616/1 and EP/G005001/1) for the funding.

References

1. B. Jaffe, W.R. Cook, H. Jaffe, *Piezoelectric ceramics* (Academic, London, 1971), pp. 135–170
2. A.H. Qureshi, G. Shabbir, D.A. Hall, *Mater. Lett* **61**, 4482–4484 (2007)
3. R.E. Eitel, C.A. Randall, T.R. Shrout, P.W. Rehrig, W. Hackenberger, S.E. Park, *Jpn. J. Appl. Phys., Part 1* **40**, 5999–6002 (2001)
4. R.R. Duan, R.F. Speyer, E. Alberta, T.R. Shrout, *J. Mater. Res* **19**, 2185–2193 (2004)
5. J.R. Cheng, W.Y. Zhu, N. Li, L.E. Cross, *Mater. Lett.* **57**, 2090–2094 (2003)
6. C.A. Randall, R. Eitel, B. Jones, T.R. Shrout, D.I. Woodward, I. M. Reaney, *J. Appl. Phys* **95**, 3633–3639 (2004)
7. M.R. Suchomel, P.K. Davies, *J. Appl. Phys* **96**, 4405–4410 (2004)
8. I. Sterianou, I.M. Reaney, D.C. Sinclair, A.J. Bell, D.A. Hall, *Appl. Phys. Lett.* **87**, 242901 (2005)
9. I. Sterianou, I.M. Reaney, D.C. Sinclair, T.P. Comyn, A.J. Bell, *J. Appl. Phys* **106**, 084107 (2009)
10. ANSI/IEEE 176–1987, IEEE Standard on Piezoelectricity (IEEE, New York, 1987).